Exp. Theo. NANOTECHNOLOGY 9 (2025) 335-346 https://doi.org/10.56053/9.S.335

Nanosensor-based satellite images and GIS filter for urban expansion analysis and its impact on climate change

*Ahmed S. Hassan, Jasim H. Kadhum, Sarmad Najah ALSalhy, Osama T. Al-Taai**

Mustansiriyah University, College of Science, Department of Atmospheric Science, Baghdad, Iraq.
*) Email: osamaaltaai77@uomustansiriyah.edu.iq

Received 21/1/2025, *Received in revised form* 3/2/2025, *Accepted* 27/2/2025, *Published* 15/3/2025

Karbala is one of the main cities in Iraq and gained its importance through religious tourism and more than three religious occasions, especially the Arbaeen visit, which brings the number of visitors to more than five million annually. Therefore, urban expansion has increased at the expense of vegetation cover and has even become a challenge for urban planning, which is the research goal. Obtaining reliable data for urban planning, evaluating, monitoring, and mapping vegetation cover and urban expansion using the Landsat-8 satellite image. Three indicators of the urban area, vegetation, and open land for five years (2003, 2010, 2015, 2020, and 2023) are used to evaluate and analyze urban expansion visually and quantitatively. In addition, some meteorological variables to evaluate the impact of urbanization on global warming in Karbala. The results show that the growth in population density has increased to reach 1,356,856 people in the year 2023, with an estimated growth rate of 1,794. This percentage is considered large when compared with other cities, and this indicates the city's recovery from the economic, commercial, and urban aspects. Remote sensing is one of the tools that can analyze satellite images. Satellite images provided from Landsat-8 and Landsat-9 were then used (NDVI) filter, and the results indicated that there is a shrinkage in agricultural areas. This contraction began to appear in 2005 in central and northern Karbala, while the largest drought the city faced was in 2015. Analysis of satellite images can estimate climate change through some meteorological variables. The results showed that the ground temperature (LST, T2M) and the air temperature at an altitude of 2 meters increased by 2ºC, and their average was (24.602, and 24.216), respectively. The noticeable increase in vertical and horizontal urban expansion compared to the shrinkage of green spaces led to verifying this fact by analyzing the images obtained and by comparing the categories of vegetation cover, which are barren, well vegetation, medium vegetation cover, and low vegetation cover. It was found that there were two categories in which their percentages were exchanged, which is the contraction of the area of vegetation cover of the wells at the expense of an increase in the low vegetation cover of 6%, especially in the last five years with the visit of visitors during the visit of Ashura and Arbaeen. This expansion is unplanned from an urban and infrastructure standpoint, so the study pointed out the difficulties accompanying it. Increasing urbanization in this particular region is associated with several notable negative consequences.

Keywords: Climate change; GIS; Population density; Nanotechnology.

1. INTRODUCTION

Nanotechnology is the manipulation of matter with at least one dimension sized from 1 to 100 nanometers. At this scale, commonly known as the nanoscale, surface area and quantum mechanical effects become important in describing the properties of matter. In light of the present ecosystem's slow but steady rise in human demands, land use/land cover (LULC) is crucial for planning and monitoring the usage of natural resources[1,2]. The significant transformations at a regional level and progress in technology have motivated academics to collect additional data. The combination of remote sensing technology and GIS tools has facilitated the monitoring of changes in land use land cover (LULC) from the past to the present. This technique has shown the alterations occurring at both the regional and global scale and has also provided significant advantages to the scientific community[3,4]. The rise of urbanization has greatly increased rural-urban migration, as it provides greater access to amenities, employment opportunities, and production facilities. Urbanization has emerged as a prominent socioeconomic concern with global implications for LULC change [5,6]. Urbanization involves the transformation of natural landscapes into areas suitable for human habitation and development. For example, Karbala has experienced a rise in urbanization because of recent economic growth and excessive population growth. The transformation has a substantial effect on the climate as buildings and roads absorb a considerable amount of solar energy both during the day and at night [7]. The evaporation rates grew in direct correlation with the rise in urbanization and the decrease in vegetation degradation. The presence of these characteristics indicates that insufficient land use planning has a detrimental impact on the regional climate[8,9].

Mapping and monitoring changes in land to use land cover (LULC) is crucial for promoting sustainable development, as well as for effective planning and management [10]. By utilizing remote sensing (RS) and geographic information systems (GIS) approaches[11,12]. An accurate understanding of the historical and contemporary condition of the land is crucial for effective environmental management [13]. This phenomenon is particularly evident in areas that are significantly influenced by fluctuations in climate and human actions. The data and condition of land use/cover (LULC) are crucial in formulating an effective and enduring environmental management program [14]. Climate change and global warming pose a significant environmental peril, particularly for arid nations. It is crucial to identify and evaluate future climate change to effectively plan for the environment and mitigate its impacts [15,16]. Climate change is a worldwide problem that impacts many regions of our inhabited globe. However, the causes and effects of climate change also vary across different regions. In Iraq, climate change is primarily caused by both anthropogenic and natural factors [17]. The significant increase in CO_2 emissions and other greenhouse gases, along with global warming, has led to drastic changes. Additionally, there has been a decrease in water inflow from rivers and streams originating from Turkey and Iran, a decline in rainfall and snowfall, and an increase in population [18,19]. All of these factors have a direct influence on the climate, leading to increasingly severe and significant effects on people's daily lives [20,21]. The measurement of Land Surface Temperature (LST) is necessary for a range of applications, including temporal analysis, global warming identification, land use and land cover assessment, water management, soil moisture calculation, and natural catastrophe monitoring. The satellite data used for estimate purposes is LANDSAT 8. The assessment of Land Surface Temperature (LST) relies on the utilization of sensor data from the Operational Land Imager (OLI) and the Thermal Infrared (TIR). The thermal band consists of spectral bands 10 and 11, which were used to evaluate land surface temperature (LST) using an algorithm [22,23]. The phenomenon of rapid urbanization has caused changes in land use and land cover, increasing land surface temperature [10]. This study aims to investigate the change that happened in Karbala by using geographic information systems (GIS) software and satellite images. The calculation of the expansion of both population density and expansion of urban planning areas and the deterioration of plant areas in the Holy Governorate of Karbala from 2005 to 2023 and their impact on changing climate factors and rising surface temperatures [24].

2. STUDY AREA AND DATASETS

Karbala city is situated south of the capital, Baghdad, at a distance of approximately 105 kilometers. The city's area is about 5560 square meters, with an elevation of 28 meters above sea level. It is situated in a strategic location that provides a direct connection to the Saudi border through Nukhayb. From the northern direction, it linked to the capital city, Baghdad. From the southern direction, it connected to Najaf. In addition, from the southeast, it connected to Hila. The city is situated at a longitude of 44° 40' and a latitude of 33° 31', as shown in Figure 1. The region is adjacent to Anbar Governorate in the north and west, Najaf Governorate in the south, and Babel Governorate in the east and northeast. The climate of Karbala is hot in summer and relatively warm in winter, and it is surrounded by palm groves and fruit trees. It takes its water from the Euphrates River. Karbala experiences a desert climate characterized by relatively high temperatures during the summer. The average of temperature occasionally reaches approximately 45 degrees Celsius at daytime, while during winter nights, it might dip to zero degrees. The city is influenced by the desert environment due to its exposure to both the desert and the alluvial plain to the east[11]. The expansion of land resulting from urban construction, population increase, and changing social and economic factors has an impact on the utilization of land. Hence, it is crucial to identify the locations where the effects of urban sprawl and its rapid expansion may be evaluated and comprehended to effectively manage Earth's surface resources for sustainable development[12,25-28].

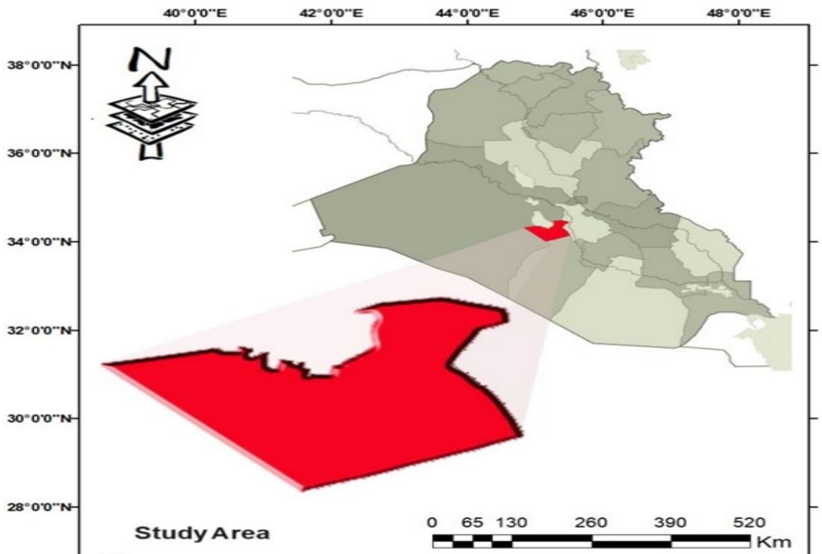

Figure 1 the geographical map of Karbala city.

The population density in the Karbala governorate has increased in the last three decades (2003 - 2023). There were many reasons for these changes. Namely, the presence of the two shrines makes it a popular and active tourist attraction. The second reason was the barbaric action in 2003, which forced people to migrate from the countryside to the city, where the population density in urban areas was 67%, while it reached 33% in the countryside as shown in table (1). Finally, these actions have affected Karbala's demography, especially increasing the numbers of people looking for jobs, as Karbala has many areas of employment that are active throughout the year. The rate of increase of population density was 1.794, with this result leading to horizontal urban expansion. Karbala has adapted to all the forces of change, expansion, and development. It was able to preserve and keep its key distinguishing characteristics by respecting the root causes of its formation. The city, thus, does have the capacity to embrace the contemporary development if it would be carefully been planned. Otherwise, if the urban expansion continues with the same negative impact, the city will completely lose its unique architectural and urban identity.

Table 1 population density for Karbala city (2003-2023).

Year	Population/person	Year	Population/person	Year	Population/person
2003	755,994	2010	1,000,546	2017	1,223,532
2004	787,072	2011	1,040,842	2018	1,239,787
2005	819,376	2012	1,082,615	2019	1,250,806
2006	852,963	2013	1,127,875	2020	1,283,484
2007	887,858	2014	1,172,938	2021	1,316,750
2008	924,085	2015	1,209,855	2022	1,354,577
2009	961,638	2016	1,215,698	2023	1,356,856

3. METHOD AND MATERIALS

Remote sensing, in conjunction with field, lithologic, structural mapping, and GIS, has significantly contributed to the investigation of regions. Remote sensing technology in the field of resource mapping. It requires comprehending the utilization of remote sensing for lithologic, structural, and alteration mapping. Remote sensing is a valuable tool for identifying deposits when the processes of mineralization create unusual spectral anomalies. Reconnaissance lithologic mapping typically serves as the initial stage in resource mapping. The study utilized imagery from Landsat 8&9 (United States Geological Survey) and data from NASA's Prediction of Worldwide Energy Resources to extract the indices areas and land surface temperature for Karbala city during the study period of July (2005, 2010, 2015, 2020, 2022). The gathered photographs were refined into a set with no clouds. The data began by downloading Landsat satellite images (Landsat -8 and Landsat 9) that consist of 11 bands, each band representing a wavelength, which enables us to calculate the indicator to analyze and process them using a geographic information system program for each of the years included in the research. The necessary adjustments were made by cutting the areas outside the study area and specifying only the desired area. Obtaining five images representing the entire borders of the governorate to analyze between the years and the geographical and urban change that occurred there due to its connection to climate change.

4. NANOSENSORS

A Nanosensor is an analytical device that incorporates a biologically active element with a suitable physical transducer to generate a measurable signal proportional to the concentration of the analyte in any type of sample. Incorporating nanomaterials into these biosensors makes them more portable, sensitive, and economical. Furthermore, with the improved detection sensitivity of nanomaterial-based biosensors, the probe material needs to be used at very low concentrations. By tuning the surface properties of the nanomaterials, these sensors can be easily used for selective and specific detection. An efficient detection system can help address many of the problems facing our modern lives.

5. RESULTS AND DISCUSSION

The Normalized Difference Vegetation Index (NDVI) is computed as the variation between near-infrared and red reflectance divided by their sum. NDVI represents smoothed NDVI observed at time step, and their ratio yields a measure of photosynthetic activity within values between. Low NDVI values indicate moisture-stressed vegetation, and higher values indicate a higher density of green vegetation. It is also used for drought monitoring and vegetation cover. This is for all five visualizations, where each visualization represents a year. Equation (1) calculations were performed on all images to extract (NDVI), a methodology employed to compute the extent of green areas in Karbala. The findings range from -1 to +1, with positive values indicating green areas and vegetative covering, while negative values are considered negligible[13]. The codes utilized for Landsat 8 and 9 to calculate the Normalized Difference Vegetation Index (NDVI) for the designated research region.

$$NDVI = (NIR\ band - Red\ band) / (NIR\ band + Red\ band) \quad (1)$$

The calculation process is carried out within a geographic information system program using the algebra function, through which the equation is applied and the results displayed directly on the images Figure 2. It was necessary to know the vegetation cover index indicating the change like the city and the decline of vegetation cover. For many reasons, the high NDVI was in 2005, then began to shrink in the following years, especially in the center and north of Karbala. While the year 2015 recorded a high rate of drought among the years of the study, the year 2022 was second in terms of drought.

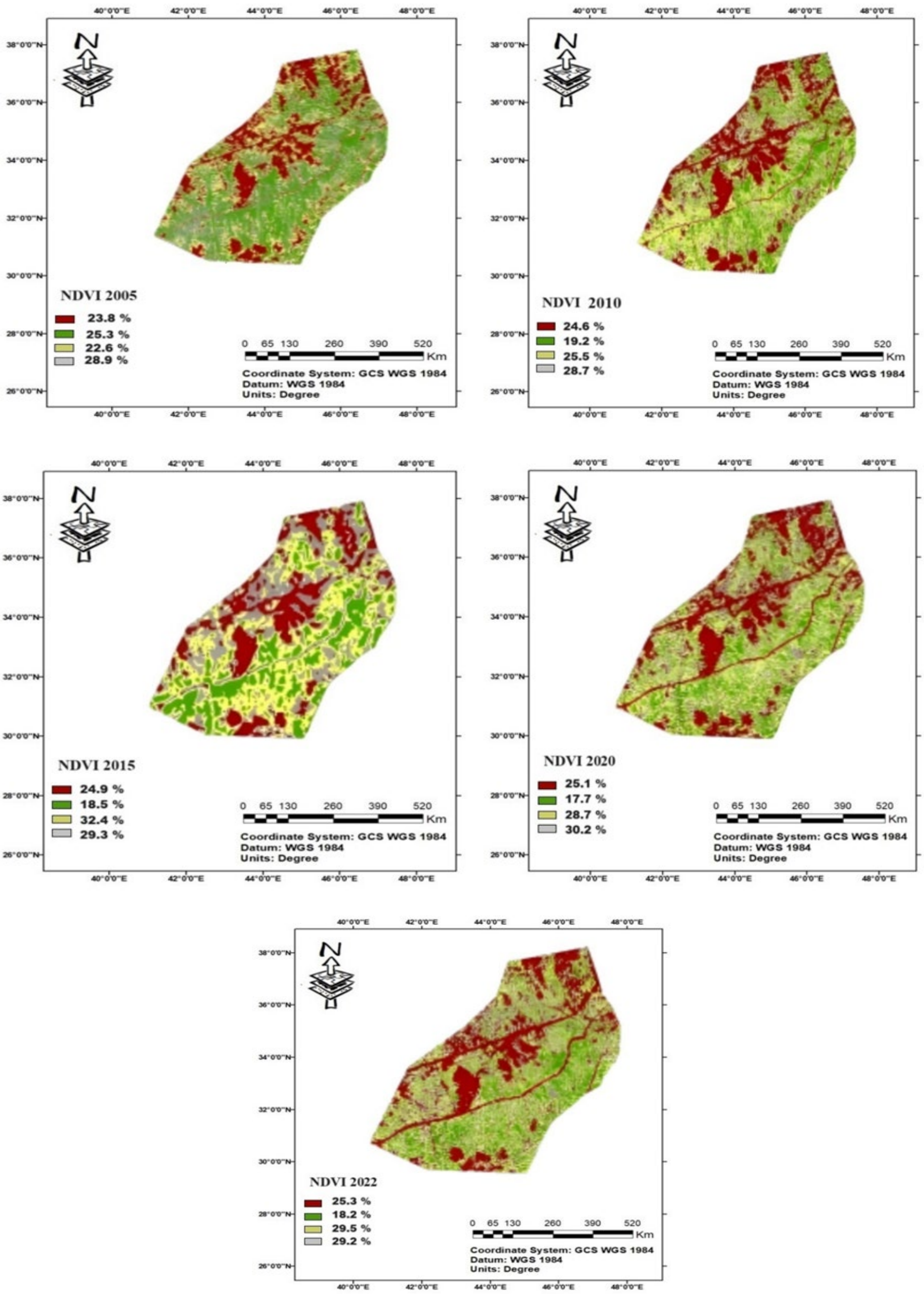

Figure 2 the growth of developed and undeveloped land and deterioration of vegetated areas.

The relationship between NDVI and some of meteorological variables; Earth's surface temperature (LST), which based on a set of equations, which based on converting to the brightness temperature at the top of the atmosphere (TOA), Equation (2). All available rewards were calculated and detailed within each band. Then, the calculation of the top-of-atmosphere brightness temperature is in equation (3).

$$BT = K2 / \ln (k1/L(\lambda) + 1) - 273.15 \quad (2)$$

$$BT = (1321.0789 / \ln (774.885 / \text{"TOA"} + 1)) - 273.15 \quad (3)$$

where *BT* Top of Atmosphere brightness temperature, ^oC in Celsius degree, *L (λ)* TOA spectral radiance, *K1: K2* constant for band#10 (from MTL txt) Kelvin (k).

In order to find out potential vegetation *(PV),* that achieved this value through calculated from extracted Land Surface Emissivity *(LSE)* from equation (4).

$$PV = ((NDVI – NDVI\ min) / (NDVImax – NDVImin))^2 \quad (4)$$

where *PV* Portion of Vegetation, *NDVI* values of NDVI image3, NDVI max/min: Max & Min values of *NDVI* image, then count it by extracting Land Surface Emissivity (E) Equation (5).

$$E = 0.004 * PV + 0.986 \quad (5)$$

where *E* Land Surface Emissivity, *PV* Portion of Vegetation.

Now, after extracting all the variables that must be available to calculate Land Surface Temperature, they will apply in Equation (6).

$$LST = BT / \{1+ (\lambda * BT / C2) * \ln (E)\} \quad (6)$$

where *BT* Top of Atmosphere brightness temperature °C, λ Wavelength of emitted radiance, For Landsat8 Band#10 λ= 10.8 and Band#11 λ=12, E Land Surface Emissivity, $C2 = h*c/s$, $C2$= 14388 mK, h Plank's constant = $6.626 * 10^{-34}$ mK, s Boltzmann constant = $1.38*10^{-23}$ JK, c velocity of light = $2.998*10^{8}$ m/s.

The computerized operations are demonstrated within the geographic information system program, and after applying all the equations, the results are displayed directly on the images (Figure 3. Moreover, with assistance data from (NASA Prediction of Worldwide Energy Resources) Data and values were obtained T2M (Temperature at 2 meters) and T2D (Dew point at 2 meters) and T2WB (Wet Bulb Temperature at 2 meters, Note the extent to which it is affected by taking place in the Karbala.

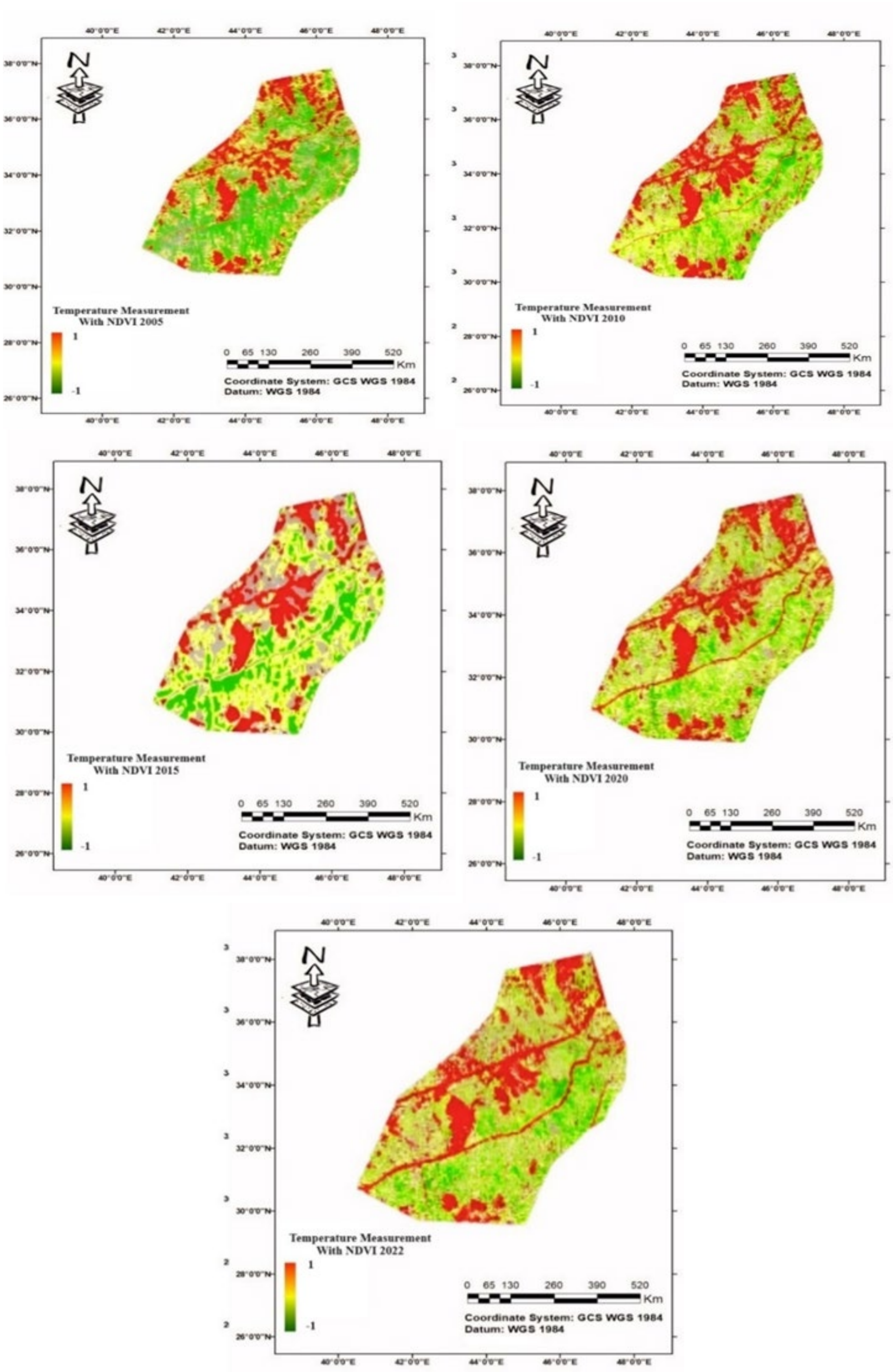

Figure 3 the Map of GIS for the land surface temperature vs NDVI in Karbala.

The application ARCGIS and the NDVI indicator were utilized to determine the overall geographical distribution of vegetative cover and built-up areas. The GIS provides colossal capabilities for dealing with large volumes of remote sensing imagery and a collection of classification methodologies used for spatial analysis via python APIs. Explore the spectral responses of built-up regions and vegetation cover, and multispectral bands from Landsat were utilized. All of the types had a unique signature in the optical bands, which indicated that they could be differentiated from the signs that were necessary for their identification. The results revealed that the urbanized areas increased dramatically after 2005, while the vegetative covered greenery spaces declined and decreased during the study period. The statistical methods namely by Standard Definition to (LST), (T2M), (T2D) and (T2WB) it became clear what percentage of increase occurred in all variables, which led to a noticeable increase in temperatures by (0.644372563) during the years of the study, as shown in Table 2.

Table 2 average and SD for some meteorological variables for Karbala during 2005-2022.

Years	Land Surface Temperature (°C)	Air Temperature at 2 meters (°C)	Dew point at 2 meters (°C)	Wet Bulb Temperature at 2 meters (°C)
2005	23.45	23.16	4.69	13.93
2010	25.38	25.04	5.96	15.5
2015	24.62	24.19	5.72	14.96
2020	24.58	24.16	6.08	15.12
2022	24.98	24.53	5.17	14.85
average	24.602	24.216	5.524	14.872
SD	0.644372563	0.615876611	0.521252338	0.51989999

When comparing the satellite images that analyzed by using the NDVI index, that significant finding out to understand that urban expansion impact and the change in Barren areas that increased, while well-vegetated areas was increased, Low green areas, Medium, and low vegetation area had less change yield less effect by urban expansion, as shown in Table 3.

Table 3 percentage of NDNI category area (2005 – 2022) in Karbala.

Years	Barren areas	Well-vegetated	Medium	Low
2005	23.80%	24.30%	28.90%	22.60%
2010	24.60%	19.20%	28.90%	25.50%
2015	24.90%	18.50%	29.30%	32.40%
2020	25.10%	17.70%	30.20%	28.70%
2022	25.30%	18.20%	29.20%	29.50%

NDVI analysis is shown in Figure 4. It is a statistical method as a pie of four categories: the barren arid region (blue), the well vegetation area (brown), the medium vegetation area (gray), and the low vegetation area (yellow) for 17 years (2005-2022). Ground cover exchange distributions between two main categories of the well vegetable area and the low vegetation area of about 6 %, exchange area wins for the low vegetation that witnessed in Karbala. The other two (barren and medium vegetation area) remained unchanged.

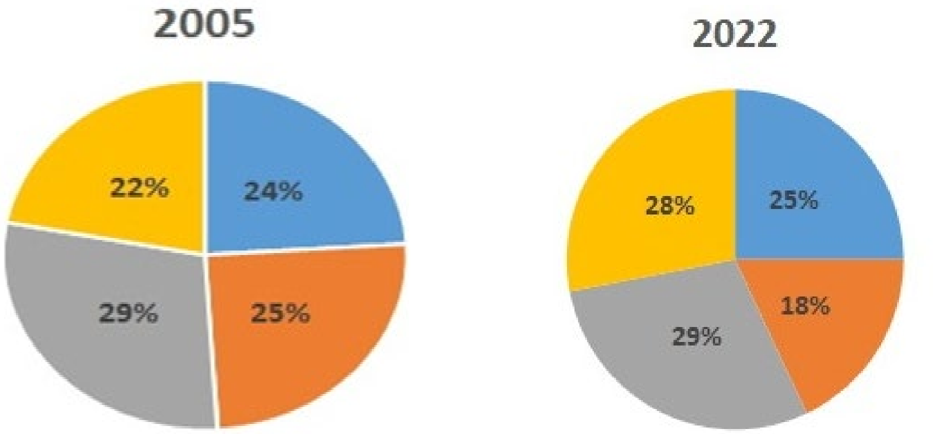

Figure 4 pie chart for NDVI during 2005-2022 in Karbala.

6. CONCLUSIONS

The main objective of this study was to analyze and study the rise in temperatures due to local urban development in Karbala and to produce an automated thematic map using the Geographic Information System service. The population of Karbala has grown significantly due to social, religious, political, and security factors, educational needs, business requirements, medical treatment, and the availability of basic infrastructure and services. Therefore, Karbala became increasingly crowded over time. Hence, large residential, commercial, and industrial areas developed to accommodate population growth and meet basic needs. The population growth increased to reach 1,356,856 people in 2023 with a growth percentage of 1.794 since 2003 that caused horizontal urban expansion. The remote sensing is a tool that can investigate the surface cover using GIS technique for the satellite image from (Landsat -8, Landsat -9) using NDVI filter. The results show that the area of vegetation cover has shrunk since 2005 in the center and north part of the city, while the south part faced a high rate of drought in 2015. This study focused on another aspect of the problem of climate change when analyzing some of the meteorological variables (LST, T2M, T2D, and T2WD). Where LST and aT2M have increased more than 2ºC, with average (24.602, 24.216) °C, respectively. The GIS plays a vital role in determining the areas of the land cover and creating thematic maps to reveal their distribution using land cover indices such as NDVI. The results showed that urbanization had a negative impact when compared among four-vegetation areas (barren, well vegetation, medium and low vegetation area). In 2005, the vegetation cover represented (25.30%) with temperatures (23.45) °C, while in 2022, the vegetation cover became (18.20%) with temperatures (24.98) °C. the NDVI analysis shown exchange distribution between two main area well vegetation area and low vegetation area about 6% toward low vegetation, while two others vegetation areas were unchanged. A disturbing fact is that uncontrolled urbanization, which leads to the destruction of vegetation and green spaces, is a significant contributor to regional warming and air pollution. This, in turn, results in the Urban Heat Island effect. It is imperative to make an effort to decrease this occurrence and concentrate on finding practical ways to alleviate its impact on both local and global warming.

7. ACKNOWLEDGMENTS

The authors gratefully acknowledge our appreciation to Mustansiriyah University for its support in completing my research. We also would like to acknowledge our appreciation to Karbala Center for Studies and Research, which supports and provides a motivating research environment for the finesse of scientific research in different fields.

References

[1] G. Vivekananda, R. Swathi, and A. Sujith, European Journal of Remote Sensing 54 (2021) 189
[2] A. H. Chughtai, H. Abbasi, and I. R. Karas, Remote Sensing Applications: Society and Environment, vol. 22 (2021) 100482
[3] A. Paarcha, Geographic Information Science for Land Resource Management 33–54 (2021) 33
[4] A. K. M. Ali and F. K. M. Al Ramahi, Iraqi Journal of Science 2142 (2020) 2149
[5] P. K. Mishra, A. Rai, and S. C. Rai, the Egyptian Journal of Remote Sensing and Space Science 23 (2020) 133
[6] Y. T. Mustafa, Environmental Remote Sensing and GIS in Iraq, 161–180 (2020) 59
[7] W. H. Hassan and B. K. Nile, Modeling Earth Systems and Environment, vol. 7 (2021) 737
[8] N. M. Abd, Z. M. Abbood, N. A. Mohammed, O. T. Al-Taai, W. G. Nassif, Nature Environment and Pollution Technology, vol. 24 (2025) 439
[9] A. Rajani and S. Varadarajan, Turkish Journal of Computer and Mathematics Education (TURCOMAT), vol. 12 (2021) 607
[10] M. A. Sresto, S. Siddika, M. A. Fattah, S. R. Morshed, and M. M. Morshed, Heliyon, vol. 8 (2022) e10309
[11] R. Abdullatif, S. R. Hammadi, and Q. Alsaady, IOP Conference Series: Materials Science and Engineering 33 (2021) 59
[12] W. G. Nassif, A. A. Hashim, S. A. Muter, O. T. Al-Taai, Asian Journal of Water, Environment and Pollution, vol. 21 (2024) 89
[13] W. G. Nassif, I. K. Al-Ataby, O. T. Al-Taai, and Z. M. Abbood, Asian Journal of Water, Environment and Pollution, vol. 21 (2024) 25
[14] J. S. A. Al Rukabie, A. S. Hassan, and J. H. Kadhum, International Journal of Advanced Science and Technology, vol. 29 (2020) 557
[15] M. H. Al-Jiboori, M. J. Abu Al-Shaeer, and A. S. Hassan, Journal of Mathematical and Fundamental Sciences, vol. 52 (2020) 353
[16] J. S. Abd Al Rukabie, A. S. Hassan, and J. H. Kadhum, IOP Conference Series: Materials Science and Engineering, vol. 928 (2020) 072048
[17] Z. M. Abbood and O. T. Al-Taai, Journal of Applied and Advanced Research, vol. 3 (2018) 128
[18] W. G. Nassif, O. T. Al-Taai, and Z. M. Abbood, IOP Conference Series: Materials Science and Engineering, vol. 928 (2020) 072089
[19] Z. M. Abbood and O. T. Al-Taai, Plant Archives, vol. 20 (2020) 822
[20] Z. M. Abbood and O. T. Al-Taai, ARPN Journal of Engineering and Applied Sciences, vol. 13 (2018) 9446
[21] S. A. Hashim, W. G. Nassif, B. I. Wahab, Z. M. Abbood, O. T. Al-Taai, Z. S. Mahdi, Journal of Engineering Science and Technology, vol. 17 (2022) 12
[22] O. T. Al-Taai, Z. M. Abbood, and J. H. Kadhum, Journal of Green Engineering, vol. 11 (2021) 779.
[23] S. A. Hashim, J. H. Kadhum, Z. M. Abbood, O. T. Al-Taai, W. G. Nassif, Nature Environment and Pollution Technology, vol. 22 (2023) 1447
[24] W. G. Nassif, F. H. Lagenean, and O. T. Al-Taai, Caspian Journal of Environmental Sciences, vol. 21 (2023) 333
[25] R. S. Al-Awadi, O. T. Al-Taai, and S. A. Abdullah, Iraqi Journal of Science, vol. 64 (2023) 4278
[26] A. M. Ahmed Alwaise, Raqeeb H. Rajab, Adel A. Mahmood, Mohammed A. Alreshedi, Exp. Theo. NANOTECHNOLOGY 8 (2024) 67
[27] Maria S. da Dunla, Exp. Theo. NANOTECHNOLOGY 8 (2024) 23
[28] Ziyad Khalf Salih, Angham Ayad Kamall-Eldeen, Exp. Theo. NANOTECHNOLOGY 8 (2024) 27

© 2025 The Authors. Published by LPCMA (https://etnano.com). This article is an open access article distributed under the terms and conditions of the Creative Commons Attribution license (http://creativecommons.org/licenses/by/4.0/).